Terabit Optical Wireless-Fiber Communication with Kramer-Kronig Receiver (Part I)

Iman Tavakkolnia, *Member, IEEE,* Cheng Chen, Yinzhou Tan, and Harald Haas, *Fellow, IEEE.*

(Invited Paper)

***Abstract*—An optical communication link is proposed for high speed point-to-point data transmission. The link incorporates both fiber and optical wireless technologies. Kramer-Kronig coherent detection is used due to its component and implementation simplicity. Spatial multiplexing, via a multi-core fiber followed by a wireless link, and wavelength division multiplexing allow the efficient exploitation of all available degrees of freedom. The link signal-to-noise ratio is estimated when all possible noise sources are taken into account. The impact of link loss and optical amplifier placement on the achievable SNR are studied theoretically. Finally, it is shown that over 1 Tb/s is achievable per wavelength with a 4-core fiber and a simple optical wireless alignment system. An important application of this design would be backhaul and intra-data center links.**

***Index Terms*—Optical Wireless Communication, Optical fiber communication, Multicore fiber, Kramer-Kronig, Data center.**

I. Introduction

Global data traffic growth has put significant pressure on all parts of digital communication systems from ultra long distance inter-continental fiber links to end-user access networks. The associated impact on data center communication links is evident owing to the fact that 90% of the global Internet Protocol traffic occurs either between different data centers or within a single data center (*i.e.*, intra-data center) [1]. Intra-data center links represent over 70% of the data traffic [2]. Therefore, it is essential to design low cost and high capacity links beyond the current solutions such as intensity-modulation direct-detection or local oscillator-based coherent systems [2].

A data center may be centralized in an infrastructure or distributed over several locations that require communication links less than 10 km [2]. The efficient utilization of power and available space in data centers is of significant importance. All-optical systems and co-packaging of the optics and electronics are proposed to reduce the system footprint and improve the energy efficiency by avoiding unnecessary electrical/optical conversions [3]. Optical wireless technology can also add the additional benefit of scalability and reconfigurability [4]–[6]. Moreover, high data rate optical wireless systems have been demonstrated experimentally [7]–[9]. While fiber links are an integral part of data center architecture for long distances between clusters of facilities, wireless links can be used for short distance connections, *e.g.*, back-haul and server connections. Therefore, an all-optical design that uses both fiber and optical wireless technologies can be beneficial for future data center networks. As a matter of fact, optical wireless communication has been thriving in recent years and is included in communication standards such as IEEE 802.15.7 and 802.11bb task groups. Light-fidelity (LiFi), which was introduced in 2011, is a network architecture based on optical wireless communication in visible and infrared spectra and encompasses all aspects of a high speed network [10], [11].

There are several options for increasing the capacity of communication links for backhaul or intra-data center connectivity, each with a corresponding technical challenge. For instance, the limited electrical bandwidth of devices imposes a symbol rate constraint on the system. The transmission power cannot be higher than certain values which are determined by the eye safety limits and maximum admissible input powers for devices. Scaling the communication network using traditional technologies, *e.g.*, intensity modulation using single-core single-mode fibers, is not desirable due to the limited space for fiber installation and pluggable transceiver connections. However, promising advances in alternative technologies, such as coherent communication, space division multiplexing (SDM) and optical wireless communication, allow us to design systems suitable for future applications such as intra-data center links.

Coherent optical communication offers increased capacity by exploiting both the intensity and phase of the optical field. Moreover, with recent advances in digital signal processing and digital/analogue converters, coherent communication with direct detection, such as Kramer-Kronig (KK), has become increasingly promising due to its smaller footprint and implementation simplicity [12]. High data rates have been demonstrated for both fiber and optical wireless data transmission [7], [13]. The other widely considered option for enhancing the capacity is increasing the number of parallel channels in wavelength and space domains. Wavelength division multiplexing (WDM) is proven to be successful and SDM is a promising solution for the next generation of optical communication systems [14]. Parallel spatial channels can be realized in a single optical fiber that incorporates multiple separate cores, known as weakly coupled multi-core fiber (MCF). For relatively short distances of intra-data center links, crosstalk is low, and thus, MCF is an suitable choice [15].

In this paper, we design a high speed fiber-wireless optical system based on wavelength multiplexed coherent communication which utilizes SDM through a MCF, followed by an optical wireless link. Coherent detection is applied by direct detection at a single photodiode (PD) and KK digital signal processing. By KK signal processing, the signal-signal beat interference (SSBI) is completely removed and the complex modulated signal is reconstructed [16]. Therefore, fiber chromatic dispersion can be compensated and the nonlinearity of

Authors are with the LiFi Research & Development Centre, Department of Electronic & Electrical Engineering, The University of Strathclyde, Glasgow, UK. e-mail: { i.tavakkolnia, c.chen, yinzhou.tan, harald.haas}@strath.ac.uk.
The work of Harald Haas was supported by EPSRC through the Established Career Fellowship under Grant EP/R007101/1, in part by The Wolfson Foundation, and in part by The Royal Society.

This is an accepted peer reviewed manuscript of the following article: Tavakkolnia, I., Chen, C., Tan, Y., & Haas, H. (2022). Terabit optical wireless-fiber communication with Kramer-Kronig receiver—Part I. IEEE Communications Letters. https://doi.org/10.1109/LCOMM.2022.3183553

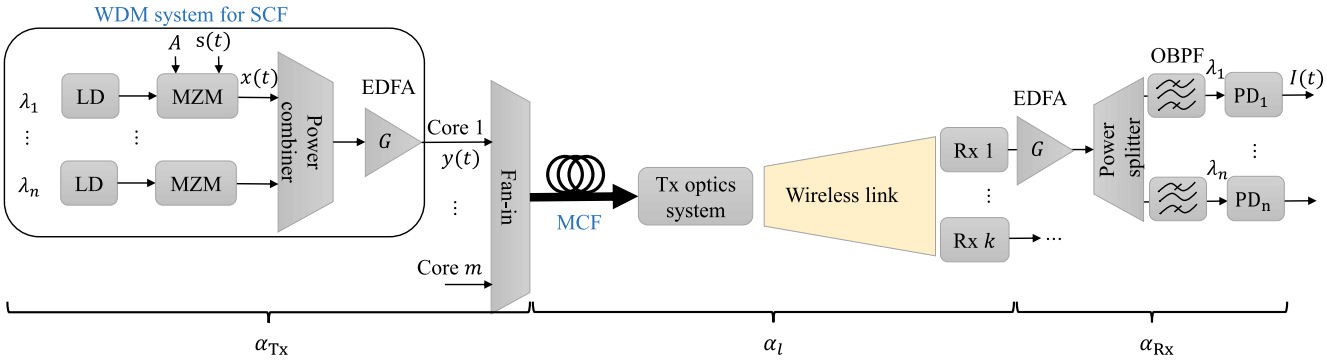

Fig. 1: The blockdiagram of the system. single core fiber (SCF), laser diode (LD), Mach-Zenhder modulator (MZM), multi-core fiber (MCF), Erbium-doped fiber amplifier (EDFA), receiver (Rx), optical bandpass filter (OBPF), photodiode (PD).

direct detection is avoided. Different noise and interference sources that affect the system are studied in this paper and the signal-to-noise ratio (SNR) is estimated. The dominant noise sources are determined by the value of link loss and the placement of optical amplifiers, *i.e.*, Erbium-doped fiber amplifier (EDFA). It is demonstrated that tera-bit-per-second data rate is achievable per wavelength with one EDFA per fiber core. In this paper, it is assumed that the link is terminated at the transmitter (Tx) and receiver (Rx) ends, however, the data modulation and detection units at the Tx and Rx can be replaced by optical switches in order to fit this link within a data center network or apply this design to other applications such as backhaul links. Part II of this work compares the system performance with intensity modulation and studies the eye-safety constraint [17].

The rest of the paper is structured as follows: In section II, the system model is presented, noise sources are introduced, and the overall link SNR is estimated. Then, the impact amplifier placement and achievable data rates are presented in section III. Finally, the paper is concluded in section IV.

II. System model

It is assumed that the interchannel interference between WDM channels is negligible, and thus the link design and performance evaluation is based on a single wavelength. Note that this assumption is perfectly valid when channels are spaced with an adequate distance between them (*e.g.*, 20 nm as in coarse WDM standard ITU-T G.694.2), and the temperature-related center wavelength shift can be ignored. The block diagram of the proposed system is depicted in Fig. 1, where an MCF is considered as the fiber communication medium followed by an optical wireless link. The fiber link for an intra-data center application can be as long as 10 km [2], and the wireless link can be used to connect servers, racks, and rows in a data center facility. We have defined equivalent loss coefficients for the transmitter, optical link, and receiver. This makes the analysis applicable to a wide range of realistic scenarios. The performance metrics can be estimated by evaluating the equivalent corresponding losses for many application scenarios. Initially, the WDM and data modulation is performed in single core fibers (SCFs). The signal is externally modulated on the optical output field of each laser diode (LD) via a phase and intensity Mach-Zenhder modulator (MZM). As the KK receiver is the basis of the transmission link, the complex optical field envelope at the output of the optical modulator can be expressed as:

$$x(t) = [A + s(t)e^{j\pi wt} + n_{\mathrm{RIN}}(t)e^{j\pi wt}]e^{jn_\phi(t)} \tag{1}$$

where $n_\phi(t)$, $n_{\mathrm{RIN}}(t)$, and $s(t)$ are respectively the phase noise, the relative intensity noise (RIN), and the baseband complex signal with power P_{s}. The amplitude of the optical carrier required for KK processing is represented by A. In (1), $w = B + 2\delta f$, where B is the signal bandwidth and δf is the frequency gap between the signal and the optical carrier [18].

Signals from all wavelength channels are then multiplexed using a power combiner. Afterwards, the combined signal can be amplified by an EDFA. The parameters of EDFA are adjusted according to the number of wavelengths and the required input power. When structure changes are required, *e.g.* scaling the data center, these parameters may be readjusted. Signals are then coupled into a MCF via a fan-in module. Therefore, the signal at the input of the corresponding core of the MCF is expressed as:

$$y(t) = \sqrt{G\alpha_{\mathrm{Tx}}}x(t) + n^{(1)}_{\mathrm{ASE}}(t), \tag{2}$$

where G is the amplifier power gain and all power losses at the transmitter are included in the parameter α_{Tx}. The amplified spontaneous emission (ASE) noise, added by the amplifier, is shown by $n^{(1)}_{\mathrm{ASE}}(t)$ which can be considered Gaussian with a variance of $\sigma^2_{\mathrm{ASE}} = n_{\mathrm{sp}}(G-1)h\nu B$, where h is the Planck constant, ν is the frequency (photon energy $h\nu$), and n_{sp} is the spontaneous emission factor. The fiber nonlinearity is ignored for the relatively short distances of the fiber (*i.e.*, less than 10 km for intra-data center links), and the effect of chromatic dispersion can be included by a linear transfer function as $y(t) * h(t)$. Note that the fiber loss is typically around 0.2 dB/km, which results in a small overall loss for the short distances considered here. The inter-core crosstalk, shown as $\mathrm{XT}(t)$, can also be regarded as an additional Gaussian noise, by assuming wide signal bandwidth, with crosstalk coefficient $N_{\mathrm{c}}\eta_{\mathrm{XT}}L$. N_{c} is the number of adjacent cores, L is the fiber length, and η_{XT} is the mean power coupling coefficient expressed as [19]:

$$\eta_{\mathrm{XT}} = \frac{2\kappa^2 R_{\mathrm{b}}}{\beta\Lambda}, \tag{3}$$

where κ is the coupling coeffient, R_{b} is the MCF bending radius, Λ is the core pitch, and β is the propagation constant.

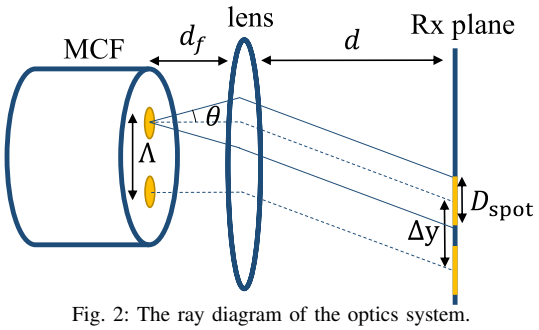

Fig. 2: The ray diagram of the optics system.

The optical field at the end of the MCF is directly sent into the wireless link using a simple optical lens system. At the receiver side, the optical signal can be coupled into another MCF and rerouted through the network. In order to reduce the alignment complexity in this paper, we design the optical system in a way that output fields from different cores are spatially separated at the receiver side (see Fig. 2). As a result, at the receiver side, another simple optical system is used to couple the optical signal originated from different cores into multiple SCFs. Fig. 2 shows the simplified ray diagram of two cores of the MCF when a lens is placed at a distance of d_f from the MCF surface, where d_f is the focal length of the lens. Using simple ray optics, the suitable focal length and spot diameter at the Rx, D_{spot}, can be found [8], [20]. The relation between the core pitch, Λ, and the separation between the spots at the receiver plane, Δy, is $\Delta y = \Lambda \frac{d}{d_f}$, where d is the distance between the lens and the receiver plane. The spot diameter is $D_{\text{spot}} = 2d_f \tan\theta$, where $\tan\theta = \lambda/(\pi\omega_0)$, where the mode field radius of the corresponding core of the MCF is ω_0. If we assume a $\Lambda = 45$ μm core pitch, $d = 10$ m, and $\omega_0 = 4$ μm, the receiver spots would have a $D_{\text{spot}} = 9.9$ mm diameter positioned $\Delta y = 1.125$ cm apart, provided that an optical lens with focal length of $d_f = 4$ cm is used. Therefore, a simple lens system can be used at the Rx to collect and collimate the optical power towards the PD. As a result, it is inferred that the described receiver structure, based on coupling the light into multiple SCFs, is feasible.

The profile of the output light of the fiber is Gaussian [21], and only the line-of-sight link is considered here. In theory, the optical wireless channel gain depends on the beam waist, link length, and detector area, but the use of lenses and the type of alignment are dominant in determining the wireless channel gain in the system shown in Fig. 1. Therefore, we consider a generic loss term α_{l} that includes losses in the fiber (including the loss due to the crosstalk), wireless link, fiber-space coupling, and optical alignment. Thus, the analysis is based on the link loss, independent of the specific link length, fiber-space coupling, or alignment method.

After coupling the optical signal into the fiber at the receiver side, another EDFA can be used to amplify the signal to the required level. A power splitter is then used to demultiplex the WDM signals. Afterwards, the signals are filtered by an optical bandpass filter (OBPF) and detected by high speed PDs. Therefore, the received electrical current at the PD is:

$$I(t) = R\alpha_{\text{Rx}}|\sqrt{G\alpha_{\text{l}}}y(t) * h(t) + \sqrt{G\alpha_{\text{l}}}\text{XT}(t) + n^{(2)}_{\text{ASE}}(t)|^2. \tag{4}$$

where α_{Rx} accounts for all the optical losses at the receiver side and R is the PD responsivity. Thermal and shot noises are not shown in (4) but will be added in the SNR expression.

A critical condition for KK processing to work is that an optical carrier must be added, digitally or optically, to the signal. The necessary and sufficient condition is that the carrier-to-signal power ratio (CSPR) should be larger than the peak-to-average-power ratio (PAPR) of the signal [16]. With this condition, the phase of a single sideband signal can be reconstructed from its intensity by applying a Hilbert transform as $\mathbf{Hilbert}[\ln(\sqrt{I(t)})]$ [16]. Without presenting the details and considering equations (1) and (2), the right-hand side of (4) can be expanded into multiple terms, where the SSBI (*i.e.*, including the square of the signal) and side band (*i.e.*, including the conjugate of the signal) components will be removed by KK processing [18]. Also, since we consider a large CSPR and low crosstalk, only the beating of crosstalk, RIN, and ASE noise with the optical carrier will be significant. Therefore, the received signal can be approximated by:

$$\begin{aligned}\hat{I}(t) \simeq\ & H|Ae^{jn_\phi(t)} * h(t)|^2 \\ & + H\{Ae^{-jn_\phi(t)} * h^*(t)\}\Big\{s(t)e^{j\pi wt+n_\phi(t)} * h(t) \\ & + n_{\text{RIN}}(t)e^{j\pi wt+n_\phi(t)} * h(t) \\ & + \frac{1}{\sqrt{G\alpha_{\text{Tx}}}}[n^{(1)}_{\text{ASE}}(t) + \text{XT}(t) + \frac{1}{\sqrt{G\alpha_{\text{l}}}}n^{(2)}_{\text{ASE}}(t)] * h(t)\Big\}\end{aligned} \tag{5}$$

where $H = RG^2\alpha_{\text{Tx}}\alpha_{\text{l}}\alpha_{\text{Rx}}$. At the receiver side, after KK processing, the effect of the channel frequency response is equalized by a simple equalization as $I(t) * h^{-1}(t)$. The first term in (5) shows the interaction of laser phase noise and chromatic dispersion. It has been shown that this term can be further simplified to an additive amplitude noise named phase to amplitude (P2A) noise [22]. The second term in (5) includes the signal itself along with the distortion caused by the phase noise (PN), equalization enhanced phase noise (EEPN), and signal-P2A beat noise (SP2A) [18]. In summary, the noise powers are given below:

$$\sigma_1^2 = \sigma^2_{\text{P2A}} = H^2A^4\int_{\delta f}^{\delta f+B} N(f)df, \tag{6}$$

$$\sigma_2^2 = \sigma^2_{\text{SP2A}} = H^2A^2P_{\text{s}}\int_{\delta f}^{\delta f+B} N(f)df, \tag{7}$$

$$\sigma_3^2 = \sigma^2_{\text{EEPN}} = H^2A^2P_{\text{s}}\pi^2|\beta_2|LB\nu_{\text{L}}, \tag{8}$$

$$\sigma_4^2 = \sigma^2_{\text{PN}} = 2H^2A^2P_{\text{s}}\pi\nu_{\text{L}}/B, \tag{9}$$

where $N(f)$ is the power spectral density of P2A noise which is a function of fiber length, chromatic dispersion parameter β_2, and laser linewidth, ν_{L} [18]. The impact of the beating of RIN, crosstalk, ASE noises with the signal and the carrier are also evident in (5). Therefore, the effective noise variances are respectively given as:

$$\sigma_5^2 = H^2A^2P_{\text{s}}(\text{RIN})B, \tag{10}$$

$$\sigma_6^2 = H^2A^2N_c\eta_{\text{XT}}LP_{\text{s}}, \tag{11}$$

$$\sigma_7^2 = H^2A^2\sigma^2_{\text{ASE}}/G\alpha_{\text{Tx}}, \tag{12}$$

$$\sigma_8^2 = H^2A^2\sigma^2_{\text{ASE}}/G^2\alpha_{\text{Tx}}\alpha_{\text{l}}, \tag{13}$$

Thermal and shot noise are also added electrically at the receiver PD. Note that the optical carrier is the dominant shot noise source, and the signal and ambient light shot noise effects can be ignored. Therefore, the additional noise powers are given as:

$$\sigma_9^2 = \sigma_{\text{Thermal}}^2 = N_0 B, \tag{14}$$

$$\sigma_{10}^2 = \sigma_{\text{Shot}}^2 = 2qHA^2B, \tag{15}$$

where N_0 is the thermal noise spectral density and q is the electron charge. Therefore, the link SNR can be calculated as:

$$\text{SNR} = \frac{H^2A^2P_{\text{S}}}{\sum_{k=1}^{10}\sigma_k^2}. \tag{16}$$

which is the most general form of the SNR. The dominant noise sources may vary depending on the situation. For instance, thermal noise is not affected by link losses, and thus, it can be the dominant noise source when the link loss is large. It should also be mentioned that noise effects, such the phase noise and inter-core crosstalk, may depend on the modulation format and some other parameters. However, it has been shown in similar works that this type of SNR estimation matches closely with experiments and realistic simulations [18], [19]. It is assumed that the channel is static for the fairly stable data center application. Thus, the channel estimation error can be ignored after an initial accurate estimation.

III. Results and Discussion

In this section, some important aspects of the system in Fig. 1 are studied. We have assumed $\alpha_{\text{Tx}} = \alpha_{\text{Rx}} = -5$ dB based on the typical losses of devices and connectors, such as power combiner/splitter, fan-in, OBPF, etc. The parameters of the system are listed in Table I. The parameters of MCFs are taken from [15]. The SNR estimation is performed based on the link loss, α_{l}, that includes the unpredictable losses over the fiber, wireless link, and connections. In other words, the results of this paper are valid for various scenarios with an equivalent link loss. Note that the MCF length is assumed as $L = 1$ km here. In Fig. 5, results for $L = 10$ km are presented which show the effect of the distortion caused by the inter-core crosstalk.

As stated earlier, signal modulation components, LD and MZM, and detection components, OBPF and PD, can be replaced by optical switches so that the system in Fig. 1 fits within a data center network. Therefore, the system can be altered to meet the requirements, such as the placement of EDFAs. Here, we show that it is sufficient to use the EDFA in either Tx or Rx without significant performance degradation. In Fig. 3, the link SNR is estimated, based on (16), for different choices of EDFA placements for a 4-core MCF at $P_{\text{s}} = -10$ dBm and CSPR $= 10$ dB. It can be seen that without any amplification the SNR is too low. If one EDFA is to be used per core, the Tx amplification results in higher SNR compared to Rx amplification, and as expected, using EDFAs at both the Tx and Rx results in the highest SNR for all link loss values. The effect of the eye-safety power constraint is discussed in part II of this work, and it is observed that a higher number of wavelengths can be used for WDM with optical amplification at Rx. Therefore, amplification at Rx results in a higher overall data rate for the full WDM system [17].

Center Wavelength	1550 nm
Bandwidth B	30 GHz
Carrier Offset δf	1 GHz
Transmitter Insertion Loss α_{Tx}	-5 dB
Receiver Insertion Loss α_{Rx}	-5 dB
PD Responsivity R	1 A/W
Amplifier Noise Figure	6 dB
Amplifier Gain G	20 dB
Spontaneous emission factor n_{sp}	1
Fiber Dispersion	16 ps/nm/km
Laser Linewidth ν_{L}	1 MHz
RIN parameter	-140 dB/Hz
Fiber length L	1 km
MCF bending radius R_{b}	50 mm
4-core MCF core pitch Λ	45 μm
7-core MCF core pitch Λ	35 μm
4-core MCF coupling coefficient κ	5×10^{-5}
7-core MCF coupling coefficient κ	35×10^{-4}

TABLE I: System parameters.

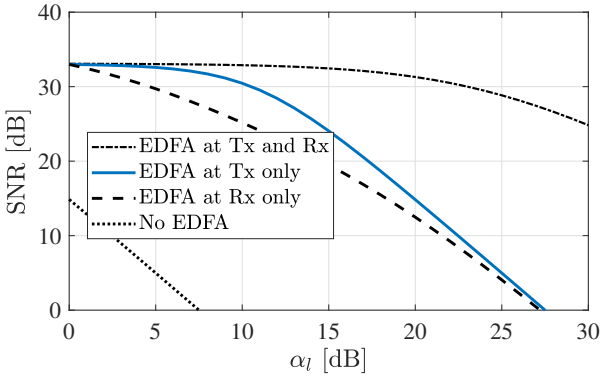

Fig. 3: SNR estimations versus link loss for different amplification strategies for a 4-core MCF at $P_{\text{s}} = -10$ dBm and CSPR $= 10$ dB.

It is insightful to understand the effect of different noise sources. Noises (6)-(10) basically originate from the Tx. Likewise, the inter-core crosstalk is dependent on the signal power at the input of MCF and effectively includes all loss parameters as in (11). The ASE noises (12) and (13) are also affected by all loss parameters, but mainly through the optical carrier beating. In order to understand the impact of different noises, the SNR is derived when only Tx noises are considered, (6)-(12), and when only Rx noises are taken into account, (13)-(15). These are compared with the true SNR, as in (16), in Fig. 4 for a 4-core MCF at $P_{\text{s}} = -10$ dBm, CSPR $= 10$ dB, and EDFA at Tx . It can be seen that the SNR is determined by the noises at Tx, when the link loss is small. Among different noise sources at Tx, the ASE, PN, and P2A noises are dominant. An increased link loss, due to various reasons, such as link length or slight misalignment, makes noises at the Rx dominant. As the received power reduces, the thermal noise becomes the main origin of distortion.

The achievable data rate is estimated as $N_c B \log_2(1+\text{SNR})$, which is an upper bound for the practical data rate. Note that it has been shown that with adaptive bit and power loading, data rates close to this bound are achievable [11]. It has been reported in recent experimental demonstrations, such as [7], that the link loss is around 5 dB. Hence, a conservative assumption for the link loss would be 10 dB. As observed in Fig. 5, over 1 and 1.5 Tb/s can be achieved at $\alpha_{\text{l}} \leq 10$ dB, respectively for a 4-core and 7-core MCF per WDM

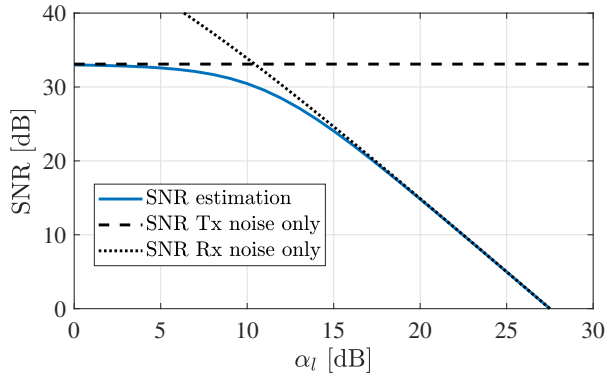

Fig. 4: The comparison of SNR estimation with the SNRs when only either Tx or Rx noises are considered for a 4-core MCF at $P_{ch} = -10$ dBm and

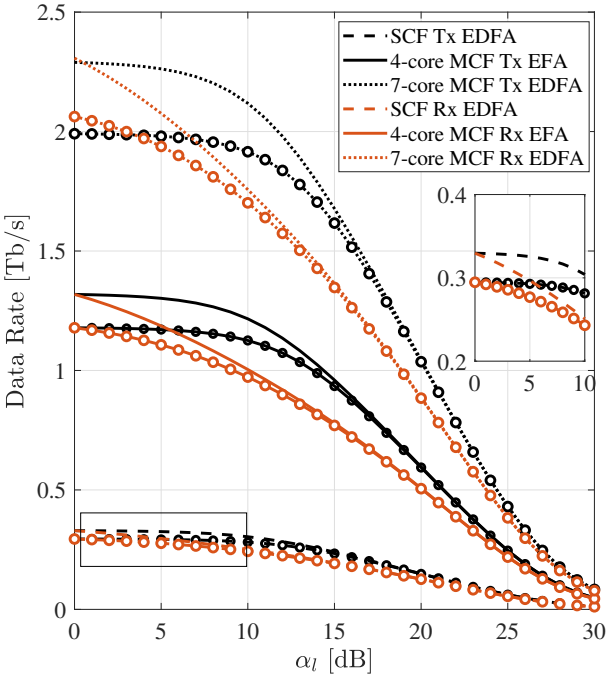

Fig. 5: Achievable data rates for SCF, 4-core, and 7-core MCFs per wavelength. Marked lines are for $L = 10$ km. The inset plot shows the magnified SCF curves. When L changes from 1 to 10 km, α_l also increases by 1.8 dB.

channel for both Rx and Tx amplification schemes. Based on a similar analysis, a SCF can achieve around 250 Gb/s. The estimated data rate values are realistic and close to the achieved values based on experimentally demonstrated results with fixed modulation formats in the literature [2], [7], [23]. For $L = 10$ km, the achievable data rate reduces due to a reduced SNR according to the analysis presented earlier. The impact of the inter-core crosstalk is dominant for 4-core and 7-core fibers. This is deduced based on the observed insignificant change in the achievable data rate of the SCF when link length increases. The final data rate of the system would be equal to the number of WDM channels times the data rate values of Fig. 5.

IV. Conclusions

Due to the inescapable necessity of high speed links for intra-data center, backhaul, and other point-to-point applications, an optical wireless-fiber link was designed and studied. Coherent communication using KK receiver and spatial multiplexing using MCF leads to high capacity of the link. Moreover, the wireless link improves the space utilization in a data center facility and potentially enables scalability and reconfigurability of the architecture. The link SNR was estimated considering all noise and distortion sources. It was also shown that tera-bit-per-second data rates are achievable per WDM channel with one EDFA per fiber core and a conservative link loss assumption of around 10 dB. The results of this paper highlight the significant potential of a hybrid fiber-wireless link structure for future applications.

References

[1] "Cisco global cloud index: Forecast and methodology, 2016–2021," White Paper, Feb., 2018.

[2] J. M. Kahn *et al.*, "Data center links beyond 100 Gb/s per wavelength," in *2020 Optical Fiber Communications Conference and Exhibition (OFC)*, Mar. 2020, pp. 1–28.

[3] B. Buscaino *et al.*, "Multi-Tb/s-per-fiber coherent co-packaged optical interfaces for data center switches," *Journal of Lightwave Technology*, vol. 37, no. 13, pp. 3401–3412, Jul. 2019.

[4] K.-T. Foerster and S. Schmid, "Survey of reconfigurable data center networks: Enablers, algorithms, complexity," *ACM SIGACT News*, vol. 50, no. 2, pp. 62–79, Jul. 2019.

[5] W. Ali *et al.*, "10 Gbit/s OWC system for intra-data centers links," *IEEE Photonics Technology Letters*, vol. 31, no. 11, pp. 805–808, 2019.

[6] S. Zhang *et al.*, "Low-latency optical wireless data-center networks using nanoseconds semiconductor-based wavelength selectors and arrayed waveguide grating router," *Photonics*, vol. 9, no. 3, p. 203, 2022.

[7] A. Lorences-Riesgo *et al.*, "200 G outdoor free-space-optics link using a single-photodiode receiver," *Journal of Lightwave Technology*, vol. 38, no. 2, pp. 394–400, Jan. 2020.

[8] T. Koonen *et al.*, "High-capacity optical wireless communication using two-dimensional IR beam steering," *Journal of Lightwave Technology*, vol. 36, no. 19, pp. 4486–4493, May, 2018.

[9] M. A. Fernandes *et al.*, "Free-space terabit optical interconnects," *Journal of Lightwave Technology*, vol. 40, no. 5, pp. 1519–1526, 2022.

[10] H. Haas *et al.*, "What is LiFi?" *Journal of lightwave technology*, vol. 34, no. 6, pp. 1533–1544, Dec, 2015.

[11] R. Bian *et al.*, "15.73 Gb/s visible light communication with off-the-shelf LEDs," *Journal of Lightwave Technology*, vol. 37, no. 10, pp. 2418–2424, May, 2019.

[12] J. C. Cartledge and A. S. Karar, "100 Gb/s intensity modulation and direct detection," *Journal of Lightwave Technology*, vol. 32, no. 16, pp. 2809–2814, Aug. 2014.

[13] S. T. Le *et al.*, "1.72-Tb/s virtual-carrier-assisted direct-detection transmission over 200 km," *Journal of Lightwave Technology*, vol. 36, no. 6, pp. 1347–1353, Mar. 2018.

[14] P. J. Winzer and D. T. Neilson, "From scaling disparities to integrated parallelism: A decathlon for a decade," *Journal of Lightwave Technology*, vol. 35, no. 5, pp. 1099–1115, Mar. 2017.

[15] H. Yuan *et al.*, "Space-division multiplexing in data center networks: on multi-core fiber solutions and crosstalk-suppressed resource allocation," *Journal of Optical Communications and Networking*, vol. 10, no. 4, pp. 272–288, Apr. 2018.

[16] A. Mecozzi *et al.*, "Kramers–Kronig receivers," *Advances in Optics and Photonics*, vol. 11, no. 3, pp. 480–517, Sep. ,2019.

[17] I. Tavakkolnia *et al.*, "Terabit optical wireless-fiber communication with Kramer-Kronig receiver (Part II)," *IEEE Communications Letters*, 2021.

[18] S. T. Le *et al.*, "A closed-form expression for direct detection transmission systems with Kramers-Kronig receiver," *IEEE Photonics Technology Letters*, vol. 30, no. 23, pp. 2048–2051, Dec. 2018.

[19] T. Hayashi *et al.*, "Uncoupled multi-core fiber enhancing signal-to-noise ratio," *Optics express*, vol. 20, no. 26, pp. B94–B103, Dec. 2012.

[20] B. E. Saleh and M. C. Teich, *Fundamentals of photonics*. john Wiley & sons, 2019.

[21] K. Wang *et al.*, "Experimental demonstration of a novel indoor optical wireless localization system for high-speed personal area networks," *Optics letters*, vol. 40, no. 7, pp. 1246–1249, Apr. 2015.

[22] S. Yamamoto *et al.*, "Analysis of laser phase noise to intensity noise conversion by chromatic dispersion in intensity modulation and direct detection optical-fiber transmission," *Journal of Lightwave Technology*, vol. 8, no. 11, pp. 1716–1722, Nov. 1990.

[23] D. Kong *et al.*, "Kramers–Kronig detection with adaptive rates for 909.5 Tbit/s dense SDM and WDM data channels," in *European Conference on Optical Communication (ECOC)*, Sep. 2018, pp. 1–3.